

Document downloaded from:

<http://hdl.handle.net/10251/104865>

This paper must be cited as:

Font-Pérez, A.; Soriano Martinez, L.; Moraes, J.; Tashima, M.; Monzó Balbuena, JM.; Borrachero Rosado, MV.; Paya Bernabeu, JJ. (2017). A 100% waste-based alkali-activated material by using olive-stone biomass ash (OBA) and blast furnace slag (BFS). *Materials Letters*. 203:46-49. doi:<https://doi.org/10.1016/j.matlet.2017.05.129>



The final publication is available at

Copyright Elsevier

Additional Information

1 **A 100% waste-based alkali-activated material by using olive-stone biomass ash (OBA) and blast**
2 **furnace slag (BFS)**

3 A. Font¹, L. Soriano¹, J. C. B. Moraes², M. M. Tashima², J. Monzó¹, M. V. Borrachero¹ and J. Payá^{1*}

4
5 ¹ICITECH – GIQUIMA Instituto de Ciencia y Tecnología del Hormigón, Universitat Politècnica de
6 Valencia, Valencia, Spain.

7 ²UNESP – Grupo de Pesquisa MAC – Materiais Alternativos de Construção. Universidade Estadual
8 Paulista (UNESP), Faculdade de Engenharia, Ilha Solteira, São Paulo, Brasil.

9 * Corresponding-author: jjpaya@cst.upv.es

10
11 **ABSTRACT**

12 This study presents the use of olive-stone biomass ash (OBA) as an alkali source in alkali-activated
13 materials (AAM) based on blast furnace slag (BFS). The OBA was physically and chemically
14 characterized. It presented high K₂O and CaO contents, and yielded high alkalinity in water medium. The
15 newly designed OBA+BFS mixes (a 100% waste-based AAM) reached a compressive strength of 30 MPa
16 after 7 days of curing at 65 °C, which was higher than for BFS activated with KOH solution.
17 Thermogravimetric studies showed the formation of C-S-H/(C,K)-A-S-H gels and hydrotalcite. The OBA
18 presented excellent performance as a component in AAM and a good valorisation was achieved.

19
20 **Keywords:** biomass ash, thermal analysis, alkali-activated material, ceramics.

21
22 **1. INTRODUCTION**

23
24 Alkali-activated materials (AAM) are prepared by mixing a solid precursor and an alkaline solution
25 (usually sodium or potassium hydroxides, carbonates or silicates). The precursor is an aluminosilicate-
26 based mineral material and in many cases this is a waste from industrial activity (e.g. fly ash, blast
27 furnace slag, ceramic wastes). Environmental benefits are provided by the use of AAMs, compared to
28 Portland cement, due to their low associated carbon footprint [1]. Alternative binder solutions also have
29 been reported by the use of mixtures of wastes, in which one of the components has a biomass waste
30 origin: sugarcane straw ash has been successfully tested in 50/50%wt mixtures with blast furnace slag [2]

31 with a significant reduction in the sodium silicate content. However, the alkaline solutions are prepared
32 by means of the use of synthetic chemical reagents, with relatively high costs in economic and
33 environmental terms. The use of alkaline wastes could help to solve this issue. In some cases, part of
34 chemical reagent has been successfully replaced by a waste (e.g. rice husk ash replaced silicate source in
35 [3]).

36 In this way, some alkaline ashes can be obtained by power generation from biomass combustion. After
37 this process, a solid by-product is generated, the biomass ash. Vassilev et al. [4] have classified these
38 biomass ashes into four types, depending on the oxides compositions: S, K, C and CK types.

39
40 The challenge of finding a use for these biomass ashes needs to be addressed. Greener concrete has been
41 developed by the use of different ashes from farming waste residues [5]. Alternatively, alkali-rich ashes
42 could be used for preparing activation solutions for AAM.

43
44 This paper presents an investigation of a waste obtained after the combustion of olive stone: olive-stone
45 biomass ash (OBA). The residue is rich in K_2O and CaO (CK ash according to [4]). Olive biomass ash
46 has already been studied in cement blends with interesting results. In these studies, the use of olive cake,
47 pulp and stone in the combustion process produced an ash with high SiO_2 content [6, 7]. Peys et al. [8]
48 studied the use of some potassium-rich biomass ashes as an activator in metakaolin mixtures, where they
49 obtained a maximum compressive strength of 40 MPa after 28 days of curing.

50
51 The aim of this research is to present the potential use of olive-stone biomass ash (OBA) as an alkali
52 source in AAMs based on blast furnace slag (BFS). The OBA was fully characterized and it was used in
53 AAM. The OBA/BFS blend was compared to water activated BFS and KOH activated BFS to assess the
54 effectiveness of OBA in the matrix development.

55

56 **2. EXPERIMENTAL**

57

58 *2.1. Materials*

59 Blast furnace slag (BFS) was supplied by Cementval (Valencia, Spain) (see Composition in Table 1) with
60 a mean particle diameter of 26.0 μm . Olive-stone biomass ash (OBA) was supplied by Almazara Candela

61 (Elche, Spain). The original ash was milled for 20 minutes in a ball mill in order to homogenise the
62 sample and to reduce the particle diameter. Commercial potassium hydroxide (KOH) was used (Panreac-
63 SA, 85% purity).

64

65 *2.2 Methods*

66 The OBA was characterized by X-ray fluorescence (XRF), pH in deionized water, particle size
67 distribution (PSD), X-ray diffraction (XRD) and field emission scanning electron microscopy (FESEM).
68 XRF was carried out using a Philips Magix Pro XRF instrument. The pH measurement was carried out by
69 means of a Crison micro PH2001 pH meter, and the PSD was measured by means of a Malvern
70 Instruments Mastersizer 2000. XRD was carried out by a Bruker AXS D8 Advance. FESEM micrographs
71 were taken by an ULTRA 55-ZEISS with the sample covered by carbon.

72

73 Three different mixes were designed in this study by using BFS as precursor, where the activating
74 solution was: a) still water without any alkali source (M1); b) an aqueous solution of KOH to produce an
75 alkali-activated material (M2); or c) the mixture of OBA and water in a 0.47 ratio (M3). The K^+ molarity
76 selected in this study was 4M for the M2. For M3, the same molarity was calculated as for the M2 based
77 on the K_2O content in the OBA: 18.8% of OBA was added with respect to the BFS. Water:BFS and
78 BFS:sand (for mortars) ratios were maintained as constant values of 0.40 and 1:3 by mass, respectively.
79 Samples were cured at 65°C and 100% relative humidity. Mortars were assessed by their compressive
80 strength (universal testing machine). Thermogravimetric analyses (TGA) of the pastes were performed
81 using a TGA850 Mettler Toledo thermobalance(temperature range: 35–500 °C; heating rate: 10 °C·min⁻¹
82 in an N₂ atmosphere. Samples were tested after 3 and 7 days.

83

84 **3. RESULTS AND DISCUSSION**

85

86 *3.1. Chemical and physical characterization of OBA*

87

88 The chemical composition of OBA is summarized in Table 1. The main oxides of the ash are K_2O
89 (32.16%) and CaO (27.77%), both significantly higher than previously reported [6]. The sum of over 60%
90 of these oxides suggests that OBA can be an important alkali source in AAMs. The OBA showed high

91 alkalinity in water suspension with a value equal to 13.5 for an OBA:water ratio of 0.47. The mean
92 particle diameter and 90%-passing diameter (d_{90}) values were 20.1 and 45.2 μm , respectively. XRD studies
93 showed that the main crystalline phases are: portlandite ($\text{Ca}(\text{OH})_2$), calcite (CaCO_3), anorthite
94 ($\text{CaAl}_2\text{Si}_2\text{O}_8$) and kalicinite (KHCO_3). FESEM images are shown in Figure 1. Fig. 1a presents the OBA
95 before the milling process. At a lower magnification, highly irregular particles with size larger than 100
96 μm can be observed. When these particles are observed at a higher magnification, they appear to have a
97 rough surface with signs of a sinterization event. Fig. 1b shows the OBA after the milling process. The
98 particle size significantly reduced when compared to the original, and a more homogeneous particle
99 distribution was observed, showing rough and smooth particle surfaces.

100

101

102

103

104

105

106 *3.2 Characterization of mortars and pastes*

107 The compressive strength for M1, M2 and M3 mortars after 3 and 7 curing days is shown in Figure 2. It is
108 noticeable that for the M3 mixture, the system is 100% waste-based material. After 3 days of curing, the
109 compressive strength for the control mortar with only water (M1) was 6.9 MPa, which corresponds to the
110 self-hydraulic properties of the BFS [9]. This value was significantly lower than those obtained for the
111 other two mortars: M2 and M3 presented 12.7 MPa and 20.6 MPa, respectively. On the one hand, these
112 results show that the alkaline activation of BFS improved the mechanical development when compared to
113 a system with only water, as expected. On the other hand, the presence of OBA in the mixture enabled it
114 to reach a compressive strength higher than that obtained in KOH alkali-activated mortar. Probably, the
115 presence of both calcium and potassium from the OBA influenced positively the activation of BFS.
116 Regarding 7-days cured mortars, M1 effectively maintained its compressive strength at 3 days, reaching
117 7.0 MPa. M2 and M3 showed a strength gain: the former mortar reached 16.9 MPa (33% gain with
118 respect to the 3 days sample) and the latter presented 29.9 MPa (45% gain). It can be noticed that the
119 presence of the OBA not only yielded the highest compressive strength, but also showed the best
120 improvement in this curing interval.

121

122

123

124

125 Thermogravimetric analyses (DTG curves) for the M1, M2 and M3 pastes after 3 and 7 days of curing are
126 shown in Figure 3. In this test, three main peaks could be observed: similar results were reported by
127 Rivera et al [10] for BFS activated by potassium hydroxide/silicate mixture. Peak 1 is related to
128 dehydration of C-S-H gel (the main peak in all pastes). Peak 2 is associated with dehydration of C-A-S-H
129 and (C,K)-A-S-H gels from the activated products. Peak 3 is only observed for the M2 and M3 pastes,
130 and is related to the dehydration of the hydrotalcite [11] (confirmed by XRD). No important difference
131 between the DTG peaks for 3 and 7 days for all pastes was observed. Regarding the relative mass losses
132 in the interval of 35–500 °C, after 3 days of curing the M2 paste presented the highest value (12.92%),
133 followed by M3 (8.35%) and M1 (4.07%). The mass losses (a measure of the chemically combined water)
134 showed significant increases from 3 to 7 days of curing because of the progress of the reaction. The
135 corresponding mass losses for 7 days of curing were M2=15.51%, M3=10.82% and M1=4.52%. This
136 behaviour can be attributed to the formation of more cementing compounds from the reaction process.
137 Curiously, the combined water for M2 is higher than that for M3, although the strength is opposite. This
138 behaviour may be due to two facts: on the one hand, the presence of more solid in the M3 mix (18.8%
139 more) achieves a filler effect in the activated matrix. On the other hand, the presence of both potassium
140 and calcium probably modifies the nature of the hydrates, making a stronger matrix.

141

142

143

144

145

146 **4. CONCLUSIONS**

147 OBA showed a high amount of calcium and potassium in its composition. In water suspension, OBA
148 produces an alkaline medium. When the OBA was reacted with BFS, the ash influenced positively the
149 compressive strength development of the mortars. After 3 and 7 days of curing time at 65 °C, this
150 OBA+BFS mix showed better strength than the corresponding KOH-activated system, suggesting a

151 synergic process in terms of the filler effect and chemical effect. The use of OBA opens an interesting
152 new line in the preparation of 100%-waste based AAMs. These results showed that new and better
153 ecological and economical materials have been designed.

154

155 **ACKNOWLEDGEMENTS**

156 Thanks are given to Almazara Candela for providing the OBA sample and BIOMASA project (UPV).

157

158 **REFERENCES**

159

160 [1] L.K.Turner, F.G.Collins, Carbon dioxide equivalent (CO₂-e) emissions: A comparison between
161 geopolymer and OPC cement concrete, *Cons. Build. Mat.* 43(2013)125-130.

162 [2] J.C.B.Moraes, M.M.Tashima, J.L.Akasaki, J.L., J.L.P.Melges, J.Monzó, M.V.Borrachero, L.Soriano,
163 J.Payá, Increasing the sustainability of alkali-activated binders: The use of sugar cane straw ash (SCSA),
164 *Const. Build. Mat.* 124(2016)148-154.

165 [3] N.Bouzón, J.Payá, M.V.Borrachero, L.Soriano, M.M.Tashima, J.Monzó, Refluxed rice husk
166 ash/NaOH suspension for preparing alkali activated binders, *Mat. Lett.* 115(2014)72-74.

167 [4] S.V.Vassilev, D.Baxter, L.K.Andersen, C.G.Vassileva, An overview of the chemical composition of
168 biomass, *Fuel* 89(2010)913-33.

169 [5] K.H.Mo, U.J.Alengaram, M.Z.Jumaat, S.P.Yap, S.C.Lee, Green concrete partially comprised of
170 farming waste residues: a review, *J. Clean. Prod.* 117(2016)122-138.

171 [6] M.Cruz-Yusta, I.Mármol, J.Morales, L.Sánchez, Use of olive biomass fly ash in the preparation of
172 environmentally friendly mortars, *ACS Envir. Sci. Tech.* 45(2011)6991-6.

173 [7] M.Cabrera, A.P.Galvin, F.Agrela, M.D.Carvajal, J.Ayuso, Characterisation and technical feasibility of
174 using biomass bottom ash for civil infrastructures, *Constr. Build. Mat.* 58(2014)231-44.

175 [8] A.Peys, H.Rahier, Y.Pontikes, Potassium-rich biomass ashes as activator in metakaolin-based
176 inorganic polymers, *App. Clay Sci.* 119(2016)401-16.

177 [9] S.C.Pal, A.Mukherjee, S.R.Pathak, Investigation of hydraulic activity of ground granulated blast
178 furnace slag in concrete, *Cem. Concr. Res.* 33(2003)1481-1486.

179 [10] O.G.Rivera, W.R.Long, C.A.Weiss Jr., R.D.Moser, B.A.Williams, K.Torres-Cancel, E.R.Gore,
 180 P.G.Allison, Effect of elevated temperature on alkali-activated geopolymeric binders compared to
 181 portland cement-based binders, *Cem. Concr. Res.*, 90(2016)43-51.
 182 [11] H.A.Abdel-Gawwad, S.Abd-el-Aleem, Effect of reactive magnesium oxide on properties of alkali
 183 activated slag geopolymer cement pastes, *Ceramics – Silikáty* 59(2015)37-47.

184

185

186

Table 1 – Chemical composition (wt%) of OBA and BFS.

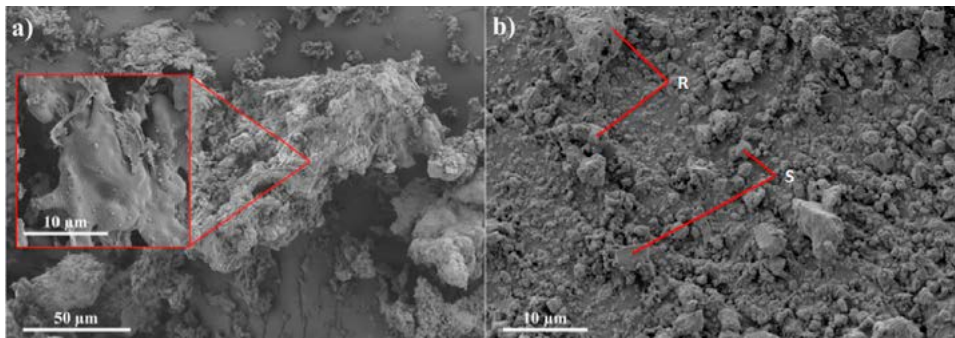
	SiO ₂	Al ₂ O ₃	Fe ₂ O ₃	CaO	K ₂ O	MgO	P ₂ O ₅	SO ₃	Na ₂ O	Others	LOI*
OBA	5.33	0.70	3.45	27.77	32.16	5.13	2.68	1.67	0.78	0.95	18.90
BFS	30.53	10.55	1.29	40.15	0.57	7.43	0.26	1.93	0.87	0.89	5.53

*Loss on ignition

187

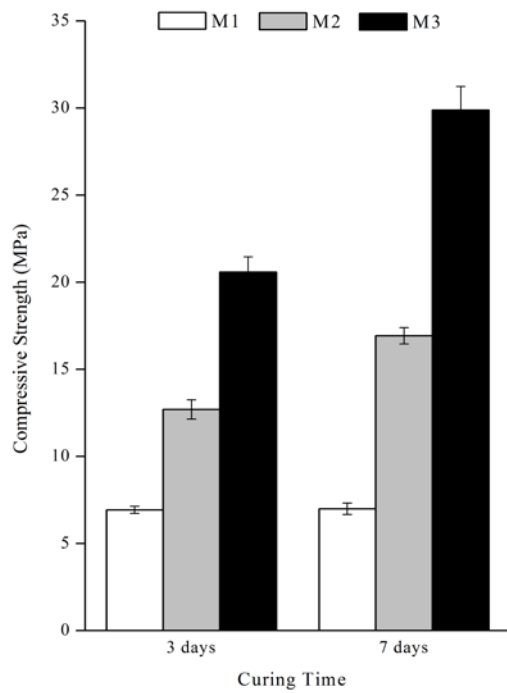
188

189



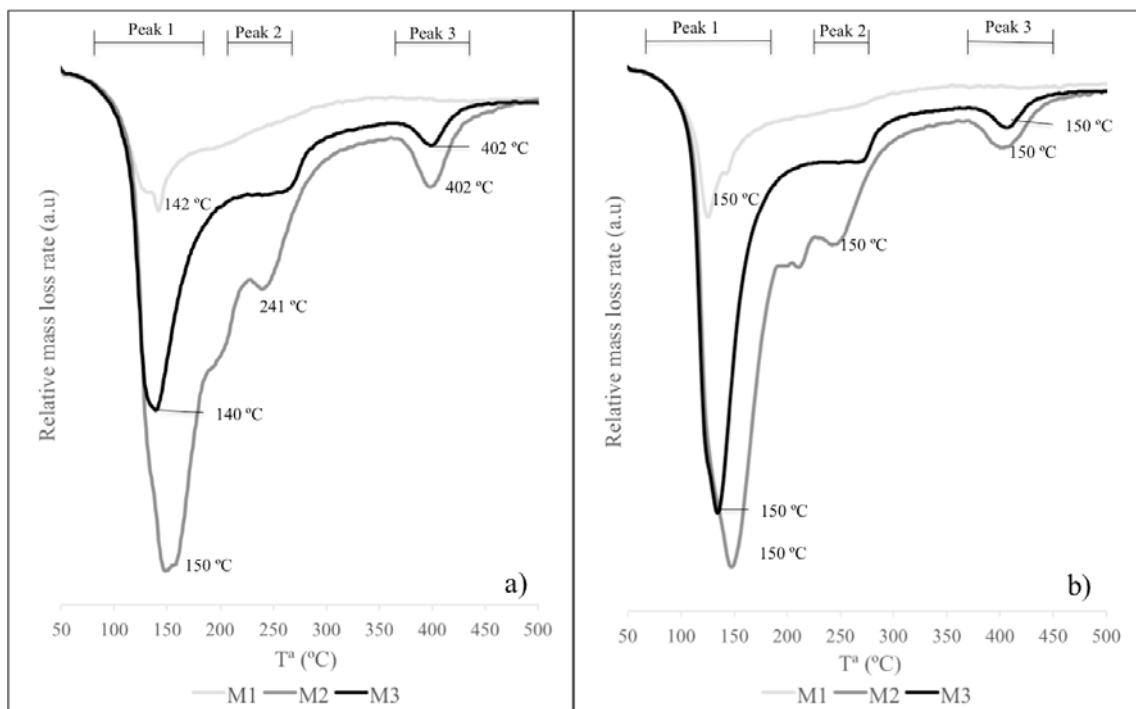
190

191 Figure 1 – FESEM micrographs of: a) original OBA; b) OBA after the milling process (R: rough surface;
 192 S: smooth surface)



193

194 Figure 2 – Compressive strength of mortars M1, M2 and M3 after 3 and 7 days of curing time at 65 °C



195

196 Figure 3 – DTG curves from pastes M1, M2 and M3 after: a) 3 days; b) 7 days of curing.

197